Enhancing Thermal Oil Heater Performance for ORC Turbines: A Comprehensive Study on Heat Transfer and Pressure Drop in Waste-to-Energy Systems

Cuk S Ali Nandar[1], Endra Dwi Purnomo[2,*], Arli Guardi[2], Harry Purnama[2], Hanna Hermawan[2], Muizuddin Azka[2], Dwi Jaya Febriansyah[2], Khamda Herbandono[2], Rudias Harmadi[2]

[1]Research Organization for Energy and Manufacture, National Research and Innovation Agency, Serpong, Indonesia, 15314
[2]Research Center for Process and Manufacturing Industry, National Research and Innovation Agency, Serpong, Indonesia, 15314

*Author to whom correspondence should be addressed:
E-mail: endr008@brin.go.id

(Received June 04, 2025; Revised August 31, 2025; Accepted December 16, 2025)

Abstract: This study investigates the thermal and hydraulic behavior of a thermal oil heater integrated into an Organic Rankine Cycle (ORC)-based waste-to-energy system, focusing on the influence of inlet air and oil mass flow rates on heat transfer and pressure drop characteristics. A series of computational fluid dynamics (CFD) simulations were conducted to analyze temperature distribution, flow dynamics, and pressure variations under varying flow conditions. The results show that increasing the inlet air mass flow rate from 0.3 kg/s to 1.3 kg/s significantly enhances convective heat transfer, raising the oil outlet temperature from 333.99 K to 385.99 K. However, higher oil mass flow rates tend to reduce this temperature gain due to shorter residence times. Statistical analysis (ANOVA) confirms the dominant influence of air flow rate on outlet air temperature ($F = 233.892$, $\eta^2 = 0.985$) and the significant effect of oil flow rate on oil outlet temperature ($F = 10.164$, $\eta^2 = 0.604$). Additionally, pressure drop analysis reveals that increased air flow rates lead to greater turbulence and higher resistance, with pressure loss rising from 85.3 Pa to 1648.5 Pa, while oil-side pressure drop remains relatively stable. These variations indicate a clear trade-off between flow conditions and system stability. Economically, higher flow configurations drastically raise operational costs, with annual energy consumption rising from IDR 133,331 to IDR 8,936,157 due to increased blower and pump power requirements. This study provides critical insights into the thermal-fluid interaction and economic implications of operating parameter variations, offering a foundation for optimizing thermal oil heater designs in ORC-based waste heat recovery systems.

Keywords: computational fluid dynamic; heat transfer; heater; organic Rankine cycle; thermal oil

1. Introduction

The utilization of thermal heater technology plays a pivotal role across various industries[1)], including manufacturing [2)], energy production [3)], and food processing [4)]. As a critical component in temperature regulation, thermal heaters are employed to ensure process stability, enhance energy efficiency, and minimize environmental impact. One innovative application of thermal heaters is in waste-to-energy power systems[5)]. In such systems, a thermal oil heater is utilized to harness waste heat generated from waste combustion using hydrodrive technology[6)]. This technology facilitates high-temperature waste incineration, converting waste into ash while producing exhaust heat that can be utilized for power generation through an Organic Rankine Cycle.

In recent years, various studies have aimed to improve the performance of ORC power plants. Fernandez et al. [7)] optimized working fluid selection to enhance efficiency, while Moradi et al. [8)] explored the influence of expander lubricating oil on micro ORC heat exchangers. Yang et al. [9)] found R717-based mixtures to be more cost-effective and thermodynamically superior to pure R717. Zheng et al. [10)]

Cite: C. Ali Nandar et al., "Enhancing Thermal Oil Heater Performance for ORC Turbines: A Comprehensive Study on Heat Transfer and Pressure Drop in Waste-to-Energy Systems". Evergreen, 12 (04) 2165-2174 (2025). https://doi.org/10.5109/7402645.

demonstrated that the heat exchanger's surface area significantly impacts system performance, and Han et al. [11] achieved system-wide cost and energy savings through integrated parameter optimization. However, despite these advancements, studies specifically targeting heat exchanger performance and cost reduction remain limited, even though this component is a major contributor to exergy loss and investment costs [10]

This study aims to evaluate the performance of a thermal oil heater under various flow rates conditions to determine the optimal configuration. The existing thermal oil heater installed in the waste-to-energy power plant, as depicted in Figure 1(a-f), exhibits certain limitations [12]. In the current air-heating configuration, heat generated from waste combustion flows through both lateral sides of a three-segment U-tube shell before being discharged horizontally. However, thermal imaging tests and performance analysis of the system reveal that the generated heat is not optimally utilized.

To address this inefficiency, a modification was implemented by truncating the U-tube[13], integrating a diffuser[14], and redirecting the airflow through the front and rear sections. Additionally, the thermal oil flow was reconfigured to enter from the top, with the outlet located at the bottom. Experimental testing on various configurations was conducted to examine the heat transfer characteristics and identify optimal conditions.

The thermal oil heater shown in Figure 1 was captured using a FLIR E95 thermal imaging camera, which has a thermal sensitivity (NETD) of <50 mK at 30 °C and an accuracy of ±2 °C or ±2%. The image indicates a maximum temperature range between 107.8 °C and 129.2 °C, with significant variations observed between the main components and the surrounding environment.. The uneven heat distribution and hot spots in the piping joints suggest potential energy losses due to inadequate thermal insulation, while sharp temperature gradients indicate possible thermal stress that may accelerate material degradation.

Moreover, unlike previous studies that mainly focused on air-side effects, this research introduces a novel finding regarding the impact of oil mass flow rate. While higher oil flow enhances circulation, it also reduces residence time, thereby limiting heat absorption a phenomenon that corresponds with findings by Giacalone et al. [15]) and Yoo [16] yet is further analyzed in our work through integrated simulation. This adds a new layer of understanding in balancing flow rate configurations for optimal performance.

These findings underscore the necessity of optimizing the inlet and outlet configurations for both the oil and hot air streams to enhance heat transfer efficiency. Improved flow distribution and thermal exchange directly contribute to the overall performance of the system, potentially increasing its thermal effectiveness and operational

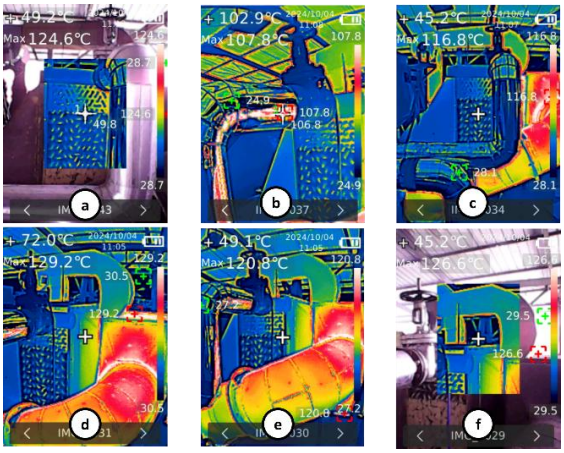

Fig. 1: Thermal imaging of existing thermal oil heater in power plan: (a) U-tube; (b) outlet diffuser; (c) wall thermal heater (d) thermal heater (side casing) (e) tube isolation (f) inlet oil

coefficient. Furthermore, this study aims to evaluate the trade-off between the operational costs associated with the use of an oil circulation pump and a hot air blower. By examining this balance, the research seeks to inform more cost-effective and energy-efficient system designs.

2. Method

The thermal distribution within the thermal oil heater, designed to cool hot air produced by waste combustion in an incinerator for Organic Rankine Cycle (ORC). The existing system circulates thermal oil through serpentine tubes while hot air flows along the outer casing. Field observations revealed significant heat loss in the piping and insulation, prompting modifications.

The heat transfer characteristics in the thermal oil heater system are governed by fundamental energy balance equations. The total heat transfer, Q is expressed as Eq.(1), where $\dot{m}$ represents mass flow rate, C_p is the specific heat capacity, and ΔT denotes the temperature difference. Specifically, for the air and oil streams, the heat transfer rates are given by Eq.(2) and Eq.(3) respectively. The logarithmic mean temperature difference (LMTD) see Eq.(4), which accounts for the varying temperature gradients along the themal heater. The overall heat transfer coefficient, U is then determined using Eq. (5) and (6), where A represents the effective heat transfer area. These equations collectively provide a comprehensive framework for analyzing and optimizing heat transfer performance, ensuring efficient energy transfer between the air and thermal oil streams, ultimately enhancing the overall system efficiency.

The redesigned system reverses the flow configuration, directing hot air through straight pipes and circulating thermal oil in the casing, flowing from a top inlet to a bottom outlet. To evaluate the performance of the modified thermal oil heater, CFD simulations were conducted to predict the thermal behavior within the system.

Cite: C. Ali Nandar et al., "Enhancing Thermal Oil Heater Performance for ORC Turbines: A Comprehensive Study on Heat Transfer and Pressure Drop in Waste-to-Energy Systems". Evergreen, 12 (04) 2165-2174 (2025). https://doi.org/10.5109/7402645.

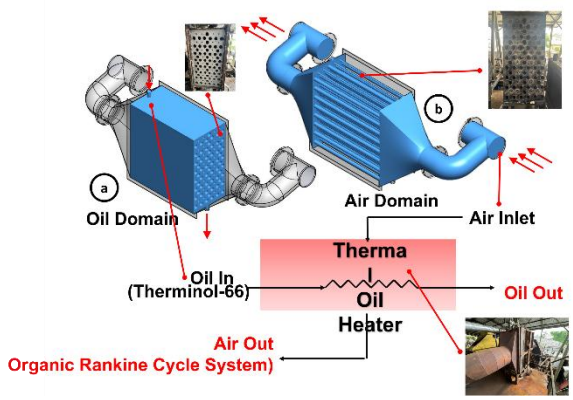

Fig. 2: Scheme of thermal oil heater flow: a) Oil Domain b) Air domain

$$Q = \dot{m} \cdot C_p \cdot \Delta T \quad (1)$$

$$Q_{air} = \dot{m}_{air} \cdot C_p \cdot \left(T_{in,air} - T_{out,air}\right) \quad (2)$$

$$Q_{oil} = \dot{m}_{oil} \cdot C_p \cdot \left(T_{in,oil} - T_{out,oil}\right) \quad (3)$$

$$\Delta T_{lm} = \frac{\Delta T_1 - \Delta T_2}{ln\left(\frac{\Delta T_1}{\Delta T_1}\right)} \quad (4)$$

$$\Delta T_1 = \left(T_{in,air} - T_{out,air}\right), \Delta T_2 = \left(T_{in,oil} - T_{out,oil}\right)$$

$$U = \frac{Q_{air}}{A_{air}(\Delta T_{lm})} \quad (5)$$

$$U = \frac{Q_{oil}}{A_{oil}(\Delta T_{lm})} \quad (6)$$

$$P = \frac{\dot{m}}{\rho} . \frac{\dot{\Delta P}}{\eta} \quad (7)$$

The simulation scheme is represented in Figure 2, and the following boundary conditions see Table 1, where Inlet mass flow to be state at a mass flow rate of 0.3080 kg/s at 673.00 K, with turbulence parameters defined by a 2% intensity and a length scale of 4.8 × 10^{-4} m. The static pressure maintained a pressure of 101,325 Pa and an ambient temperature of 293.20 K, with turbulence properties consistent with those of the inlet. The simulations were conducted under steady-state conditions to model fluid flow and heat transfer. Simulations analyzed air (0.3–1.3 kg/s) and thermal oil (0.3–1.2 kg/s), evaluating temperature distribution, fluid flow patterns, and pressure drops. Geometries and boundary conditions mirrored field setups, ensuring reliable representation. The study highlights key performance improvements in temperature distribution and pressure gradients following design modifications.

Table 1: Boundary condition

Parameters	Inlet Mass Flow (oil)
Flow	Mass flow rate: (Parameter Set Up)
Thermodynamic	Approximate Pressure: 101325.00 Pa Initial Temperature : 673.00 K
Turbulence	Intensity: 2.00 %, Length: 4.800e-04 m
Boundary layer	Layer type: Turbulent
Inlet Mass Flow (air)	
Flow	Mass flow rate: (Parameter Set Up)
Thermodynamic	Temperature Type: Temperature of Initial components Temperature: 303.00 K
Turbulence	Intensity: 2.00 %, Length: 4.800e-04 m
Boundary layer	Layer type: Turbulent
Outlet (Oil)	
Thermodynamic	Environment pressure: 101325.00 Pa Initial Temperature: 293.20 K
Turbulence	Intensity: 2.00 %, Length: 4.800e-04 m
Boundary layer	Layer type: Turbulent
Outlet (Air)	
Thermodynamic	Static pressure: 101325.00 Pa Temperature type: Temperature of initial components Temperature: 293.20 K
Turbulence	Intensity: 2.00 %, Length: 4.800e-04 m
Boundary layer	Layer type: Turbulent

The computational mesh was generated using Flow Simulation Meshing with a structured tetrahedral grid. To accurately capture near-wall phenomena, boundary layer effects were resolved using inflation layers, with the first cell height selected to ensure a non-dimensional wall distance of $y^+ < 1$. Mesh refinement was applied in regions of high gradient sensitivity, particularly around the tubes and at the inlet and outlet. The final mesh consisted of approximately 85120 elements.

3. Results

The simulation results for the thermal oil heater performance reveal a significant interplay between inlet air and oil mass flow rates on temperature outputs and pressure drops. As the inlet air mass flow rate increased from 0.3 kg/s to 1.3 kg/s, and the oil mass flow rate varied from 0.3 kg/s to 1.2 kg/s, a noticeable trend in the outlet oil temperatures was observed, with a peak temperature of 385.99 K at the highest mass flow rate combination. Concurrently, the pressure drop across the oil and air domains exhibited systematic variations, reflecting the dynamic response of the system under different operational conditions. These findings underscore the critical role of flow rate optimization in achieving enhanced thermal performance and pressure stability in waste-to-energy systems utilizing organic Rankine cycle (ORC) turbines.

Cite: C. Ali Nandar et al., "Enhancing Thermal Oil Heater Performance for ORC Turbines: A Comprehensive Study on Heat Transfer and Pressure Drop in Waste-to-Energy Systems". Evergreen, 12 (04) 2165-2174 (2025). https://doi.org/10.5109/7402645.

Figure 3 and Figure 4 present the ANOVA results, demonstrating that both air and oil mass flow rates significantly influence the thermal performance of the system. Specifically, the inlet air mass flow rate has a highly significant effect on the outlet air temperature ($F = 233.892$, $p < 0.001$), accounting for 98.5% of the variance (partial $\eta^2 = 0.985$), while the oil mass flow rate significantly affects the outlet oil temperature ($F = 10.164$, $p < 0.001$), explaining 60.4% of the variance (partial $\eta^2 = 0.604$). These results strongly reject the null hypotheses and confirm that both parameters are critical in optimizing heat transfer efficiency within the thermal system.

The increase in inlet air mass flow rate significantly enhances convective heat transfer efficiency in thermal oil heaters, resulting in higher outlet temperatures for both air and oil. This effect is driven by increased flow turbulence, which improves the heat transfer coefficient on the air side and accelerates energy transfer to the oil[17]. However, higher oil mass flow rates moderate the rise in oil outlet temperature due to the greater thermal capacity. Studies indicate that higher flow rate improve heat transfer efficiency by 30-50%, with turbulence playing a critical role in reducing thermal resistance at fluid boundaries [18,19]. These findings underscore the need for optimizing air and oil mass flow rates to achieve maximum thermal performance.

An increase in inlet air mass flow rates significantly enhances the oil outlet temperature, particularly at lower oil flow rate, due to the improved convective heat transfer rate resulting from the reduced thermal boundary layer thickness[20]. Higher inlet air accelerates fluid movement, reduces the thermal boundary layer, and improves energy transfer efficiency[21]. For instance, at an air of 0.3 kg/s and an oil of 0.3 kg/s, the oil outlet temperature was recorded at 333.99 K, while at an air of 1.3 kg/s under the same oil mass flow rate condition, the temperature increased to 385.99 K. Conversely, an increase in oil flows shortens the residence time between the oil and hot air, limiting the oil's ability to absorb heat effectively. This indicates that higher oil flow rate reduces the heat transfer effectiveness. These findings align with those of [16,22,23] which demonstrate that higher fluid flow rate in turbulent flows enhance heat transfer efficiency, although residence time remains a critical factor in determining overall heat transfer performance.

The provided simulation results as shown in Figure 5 and Figure 6, represented by the outlet air and oil total pressure versus iterations graph, indicate convergence across all test cases. Each curve demonstrates a stabilization of total pressure after approximately 200 iterations, signifying that the solution has reached steady-state conditions. The absence of significant fluctuations or oscillations in pressure values after convergence points ensures the numerical accuracy and stability of the simulation. This level of convergence confirms that the results are reliable and can be confidently used for further analysis of thermal oil heater performance under varying inlet air and oil flow conditions[24].

The variation of inlet air and oil mass flow rate in the thermal oil heater system significantly impacts heat transfer, pressure drop, and flow turbulence within the tubes[25]. Test results indicate that increasing the air inlet mass flow rate enhances the oil outlet temperature. For instance, at Inlet Air 0.75 kg/s/Oil 0.3 kg/s, the oil temperature reaches 365.7 K, compared to 344 K at Inlet Air 0.4 kg/s/Oil 0.3 kg/s, due to intensified convective heat transfer as the thermal boundary layer becomes thinner[26,27]. However, higher oil flow rate, such as at Inlet Air 1.0 kg/s/Oil 1.2 kg/s, reduce the oil outlet temperature from 376 K to 323 K, as the shorter residence time of the oil limits its ability to absorb heat effectively[28]. Air pressure drop (see Figure 7) increases with rising air inlet flow rate, from 85.3 Pa at Inlet Air 0.3 kg/s/Oil 0.3 kg/s to 1648.5 Pa at Inlet Air 1.3 kg/s/Oil 0.3 kg/s, indicating higher turbulence due to an increased Reynolds number[29,30]. In contrast, the oil pressure drop (see Figure 8) remains relatively stable, with minimal variation, showing that oil mass flow rate has a less significant effect on pressure drop [31]. This phenomenon underscores that the highest heat transfer efficiency occurs with a combination of high air inlet mass flow rate and low oil flow rate, which maximizes convective heat transfer and minimizes system

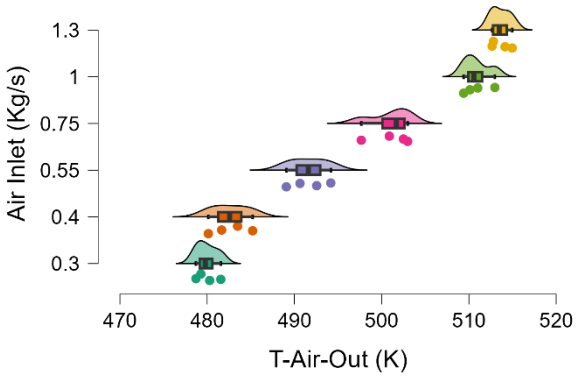

Fig. 3: Air Outlet Temperature (K)

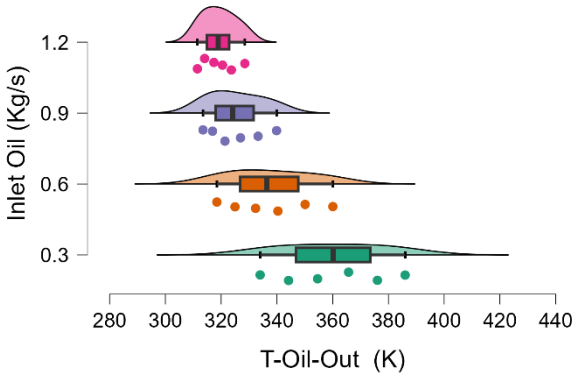

Fig. 4: Oil Outlet Temperature (K)

Cite: C. Ali Nandar et al., "Enhancing Thermal Oil Heater Performance for ORC Turbines: A Comprehensive Study on Heat Transfer and Pressure Drop in Waste-to-Energy Systems". Evergreen, 12 (04) 2165-2174 (2025). https://doi.org/10.5109/7402645.

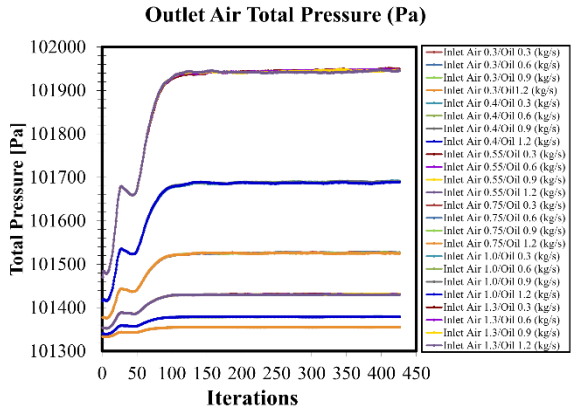

Fig. 5: Outlet Air Total Pressure

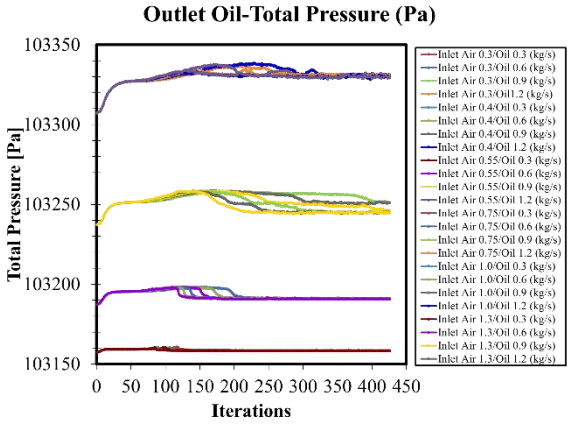

Fig. 6: Outlet Oil Total Pressure

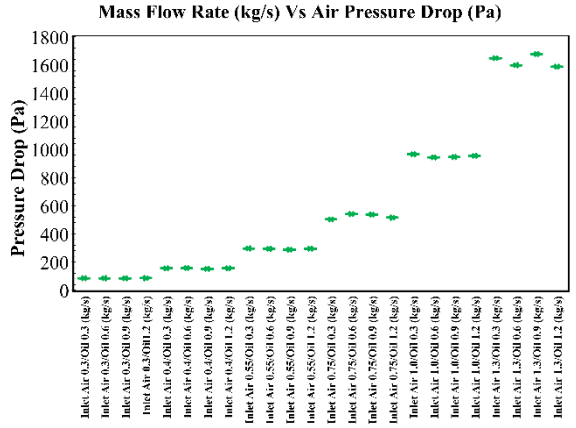

Fig. 7: Air Pressure Drop

pressure losses[32]. These findings provide critical insights for optimizing thermal oil heater designs, reducing energy losses due to pressure drops, and improving heat transfer efficiency.

The temperature distribution in the heat transfer system indicates that the oil flow rate plays a dominant role in enhancing thermal efficiency compared to the fixed air flow rate (0.3 kg/s). At low oil flow rates (0.3 kg/s), the predominance of red areas signifies limited cooling capacity, while high oil flow rates (1.2 kg/s) result in a predominance of blue areas, reflecting maximum heat

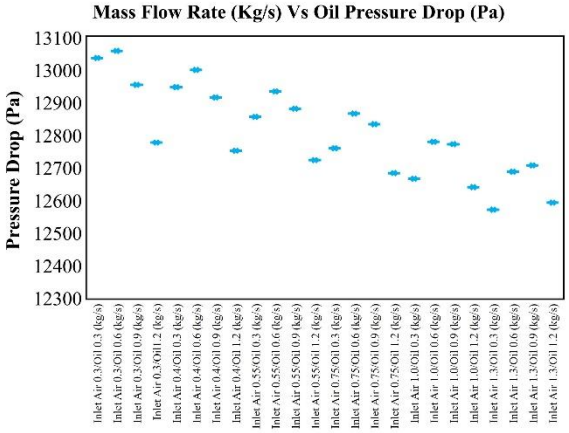

Fig. 8: Oil Pressure Drop

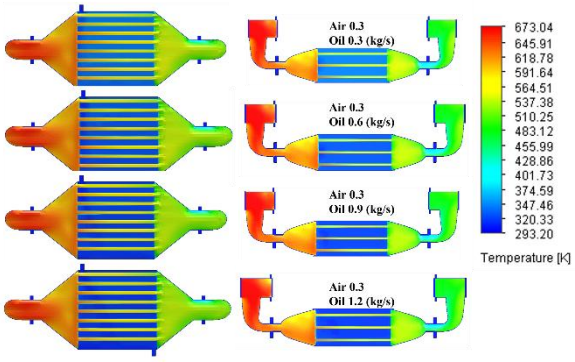

Fig. 9: Temperature of 0.3 kg/s air and 0.03-1.2 kg/s oil

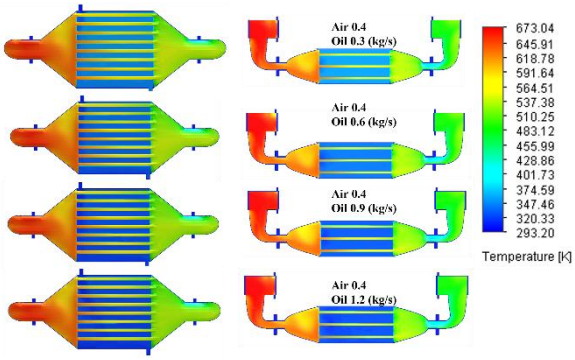

Fig. 10: Temperature of 0.4 kg/s air and 0.2-1.2 kg/s oil

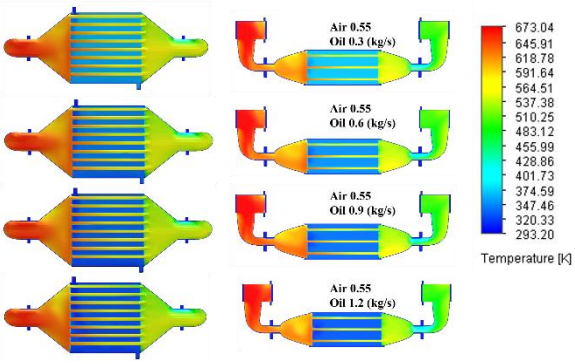

Fig. 11: Temperature of 0.55 kg/s air and 0.3-1.2 kg/s oil

transfer through increased convective capacity. The more uniform temperature gradient at higher oil flow rates

indicates consistent heat absorption along the length of the thermal oil heater, even as the total heat transfer increases. At an initial air mass flow rate of 0.3 kg/s (Figure 9), the system exhibits pronounced axial temperature gradients and elevated oil outlet temperatures, a direct consequence of extended oil residence times and insufficient air-side convective conductance. Incremental increases to 0.4 kg/s (Figure 10) and 0.55 kg/s (Figure11) demonstrate a progressive stabilization of the temperature field and the onset of a transitional regime, where the homogenization of thermal profiles indicates a significant reduction in the interfacial thermal resistance between the fluid streams. Further augmentation of the airflow to 0.75 kg/s (Figure 12) and 1.0 kg/s (Figure 13) shifts the system toward a state of dominant forced convection, achieving maximum thermal uniformity and minimum oil exit temperatures; however, the latter reveals a critical performance trade-off

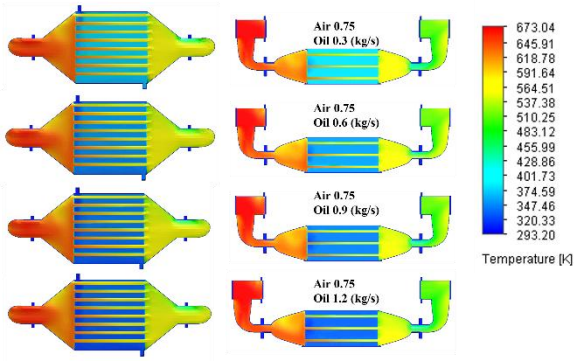

Fig. 12: Temperature of 0.75 kg/s air and 0.3-1.2 kg/s oil

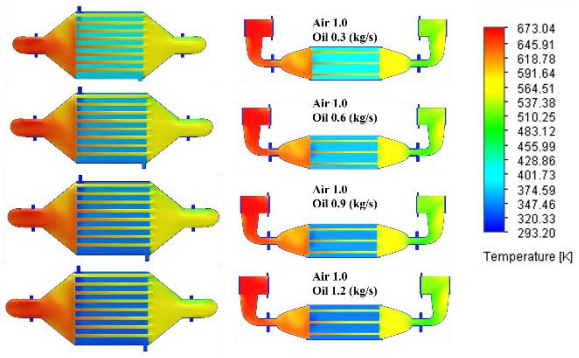

Fig. 13: Temperature of 1.0 kg/s air and 0.3-1.2 kg/s oil

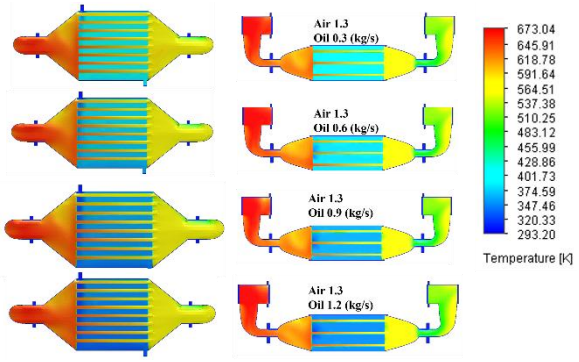

Fig. 14: Temperature of 1.3 kg/s air and 0.3-1.2 kg/s oil

for Organic Rankine Cycle (ORC) applications, as the suppression of oil temperature gain limits the available exergy for the downstream power cycle. The parametric sensitivity shown in Figure 14 highlights a thermal saturation threshold where increasing oil mass flow rates outpace the heater's dissipation capacity even under peak airflow conditions. This mechanism is fundamentally explained by the cross-sectional analysis in Figure 15, where low airflow velocities (0.3–0.55 kg/s) fail to penetrate the viscous oil core, resulting in persistent high-temperature zones throughout the channels. In contrast, optimization of the airflow to 1.3 kg/s (Figure 16) effectively overcomes these radial thermal resistances by establishing steep radial temperature gradients, thereby ensuring robust core cooling and stable operational integrity even at maximum oil flowrates. The heat transfer performance progressively improves, as evidenced by the enhanced uniformity of temperature distribution and greater dominance of blue areas across the thermal oil heater[33]. This emphasizes that higher oil flow rates enhance the system's thermal capacity, though they may also increase pressure and pumping costs[34,35]. Design optimization is therefore essential to balance heat transfer efficiency and energy consumption, as noted by[36]. The thermal efficiency of heat transfer systems is highly dependent on operational parameters such as fluid flow rate, which influences the rate of heat transfer and temperature distribution[37]. Based on Figure 17 the heat

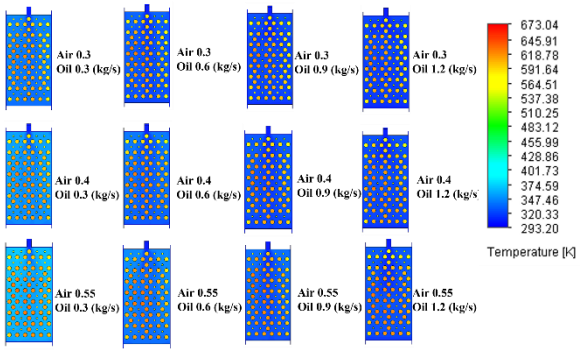

Fig. 15: Cross Section view of 0.3-0.55 kg/s air and 0.3-1.2 kg/s oil

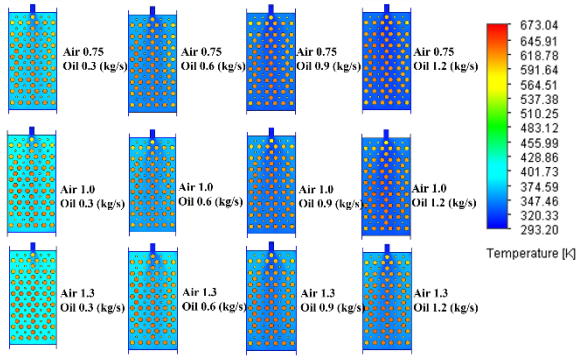

Fig. 16: Cross Section view of 0.75-1.3 kg/s air and 0.3-1.2 kg/s oil

Cite: C. Ali Nandar et al., "Enhancing Thermal Oil Heater Performance for ORC Turbines: A Comprehensive Study on Heat Transfer and Pressure Drop in Waste-to-Energy Systems". Evergreen, 12 (04) 2165-2174 (2025). https://doi.org/10.5109/7402645.

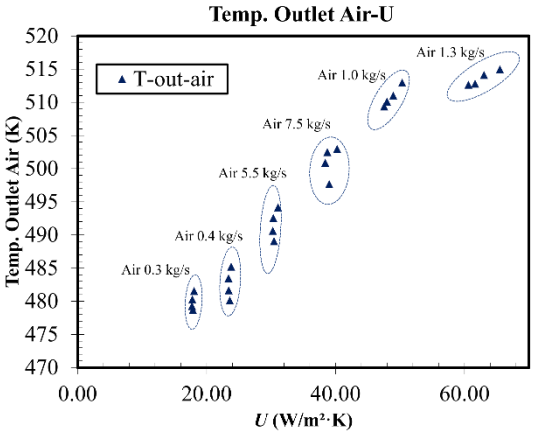

Fig. 17: Temperature of air outlet vs heat transfer coefficient

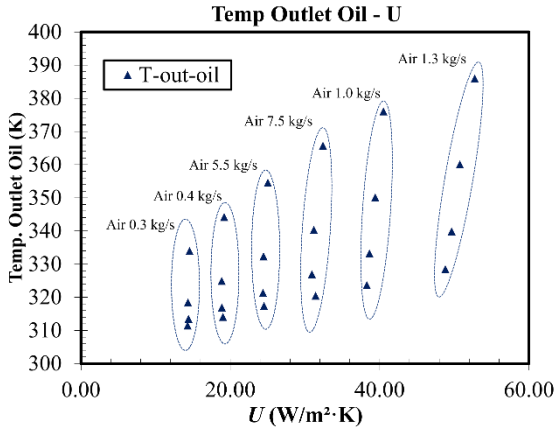

Fig. 18: Temperature of oil outlet vs heat transfer coefficient

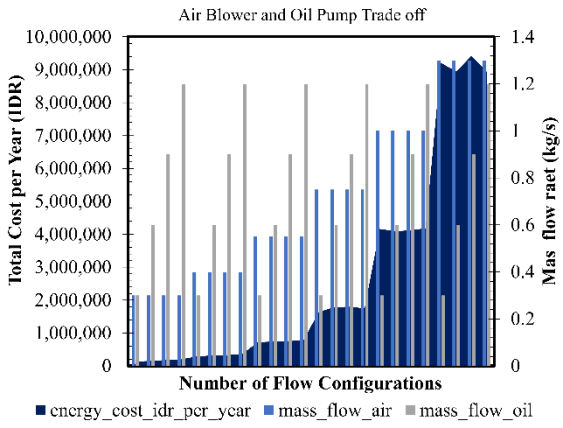

Fig. 19: trade off-cost of year of blower and pump

transfer coefficient and outlet air temperature reflects convective heat transfer dynamics in the thermal oil heater exhaust system[38]. In the circled region, where inlet air mass flow rate remains constant, the heat transfer coefficient is relatively stable despite temperature variations, indicating that heat transfer is primarily governed by exhaust gas thermal conductivity and flow turbulence rather than temperature alone[39]. Outside this region, temperature variations significantly influence the heat transfer coefficient, suggesting increased heat transfer due to fluid viscosity changes, temperature gradients, or enhanced forced convection [40]. This aligns with convective heat transfer principles, where heat transfer rates increase with higher fluid flows and greater temperature differentials [41].

The heat transfer coefficient remains stable within the circled region, see Figure 18 where inlet air mass flow rate is constant, indicating that factors like oil thermal conductivity and flow characteristics dominate heat transfer.

The analysis reveals a significant economic trade-off resulting from increased air mass flow rates within the system, see Figure 19. An increase in airflow from 0.3 kg/s to 0.4 kg/s, while maintaining a constant oil flow, leads to a more than twofold rise in annual energy costs, despite only minor changes in system parameters. This indicates that improvements in thermal performance do not necessarily translate into economic efficiency, primarily due to the substantial rise in blower power consumption. This trend becomes more pronounced in the extreme configuration of 1.3 kg/s air flow and 1.2 kg/s oil flow, where the annual operational cost reaches IDR 8,936,157 These findings underscore the necessity of identifying an optimal operating point that balances thermal performance with energy efficiency, thereby supporting the long-term sustainability of the system[15].

4. Conclusions

This study comprehensively investigated the thermal and hydraulic performance of a thermal oil heater integrated into an Organic Rankine Cycle (ORC)-based waste-to-energy system, with a focus on optimizing the inlet-outlet configuration and evaluating the trade-off between heat transfer efficiency and operational cost. The simulation results demonstrate that both air and oil mass flow rates significantly influence temperature distribution, heat transfer coefficients, and pressure drop characteristics.

Notably, increasing the air mass flow rate from 0.3 kg/s to 1.3 kg/s markedly enhances convective heat transfer and elevates outlet oil temperatures, with the highest recorded value reaching 385.99 K. However, higher oil flow rates tend to moderate this temperature gain due to increased thermal capacity and reduced residence time. Statistical analysis using ANOVA confirms the dominant influence of airflow on air-side heat transfer ($\eta^2 = 0.985$) and the significant role of oil flow on oil-side performance ($\eta^2 = 0.604$).

Furthermore, the pressure drop analysis reveals that rising air flow intensifies turbulence and resistance, elevating blower energy demands, while oil-side pressure drop remains relatively stable. These hydraulic behaviors directly impact energy consumption. Economic analysis shows a sharp increase in annual energy cost—from IDR

133,331 at low airflow conditions to over IDR 8.9 million at high flow settings—highlighting a clear trade-off between thermal performance and operational expense. Therefore, while high air and oil flow rates improve heat transfer, they simultaneously escalate pumping and blower power requirements, reducing overall economic efficiency. In conclusion, this research emphasizes the importance of identifying an optimal operating range that balances thermal effectiveness with energy consumption. Such multi-objective optimization is essential for maximizing system performance while minimizing operational costs, thereby supporting the design of sustainable, cost-effective waste heat recovery systems for ORC applications.

Acknowledgements

The authors express sincere gratitude to the Indonesia Endowment Fund for Education (LPDP) Ministry of Finance Indonesia, grant no PRJ-30/LPDP/2020, and BRIN research grant 2024 for funding this research under the 2026 Sustainable Program for the Integration of Waste-to-Energy Power Generation. We sincerely thank PT. Bumiresik Nusantara Raya for supporting this research through its waste-to-energy facilities, contributing to the thermal analysis of the thermal oil heater in power generation.

Nomenclature

Q	heat transfer rate (W)
$\dot{m}$	mass flow rate (kg/s)
C_p	specific heat at constant pressure J(kg.K)
$T_{in,air}$	inlet temperature of air (K)
$T_{out,air}$	outlet temperature of air (K)
$T_{in,air}$	inlet temperature of air (K)
$T_{out,oil}$	outlet temperature of oil (K)
ΔT_{lm}	log mean temperature difference (LMTD)
ΔT_1	temperature difference of air inlet-outlet (K)
ΔT_2	inlet temperature of oil inlet-outlet (K)
U	overall heat transfer coefficient (W/m^2.K)
ΔP	pressure drop (Pa)
η	pump and blower efficiency

References

1) R. Flores-Quirino, O. Pastor-Reyes, J.P. Aguayo, G. Ascanio, F. Méndez, J.F. Hernández-Sánchez, and S. Sánchez, "Thermal impact induced by the environment in the transport of heavy oils in offshore insulated pipelines: evaluation of heat transfer," J Pet Sci Eng, 217 110819 (2022). doi:10.1016/j.petrol.2022.110819.
2) Y. Ding, W.K. Chiu, and X.L. Liu, "Numerical investigation on thermal response of oil-heated tool for manufacture of composite products," Compos Struct, 47 (1–4) 491–495 (1999). doi:10.1016/S0263-8223(00)00028-3.
3) F. Sahin, and L. Namli, "Thermal performances and stabilities of nanofluids in an electrical oil heater," J Therm Anal Calorim, 145 (6) 3195–3206 (2021). doi:10.1007/s10973-020-09826-1.
4) J.G. Brennan, and A.S. Grandison, eds., "Food Processing Handbook," Wiley, 2011. doi:10.1002/9783527634361.
5) O.E. Medina, C. Olmos, S.H. Lopera, F.B. Cortés, and C.A. Franco, "Nanotechnology applied to thermal enhanced oil recovery processes: a review," Energies (Basel), 12 (24) 4671 (2019). doi:10.3390/en12244671.
6) I. Dolianitis, D. Giannakopoulos, C.-S. Hatzilau, S. Karellas, E. Kakaras, E. Nikolova, G. Skarpetis, N. Christodoulou, N. Giannoulas, and T. Zitounis, "Waste heat recovery at the glass industry with the intervention of batch and cullet preheating," Thermal Science, 20 (4) 1245–1258 (2016). doi:10.2298/TSCI151127079D.
7) A. Fernández-Guillamón, Á. Molina-García, F. Vera-García, and J.A. Almendros-Ibáñez, "Organic rankine cycle optimization performance analysis based on super-heater pressure: comparison of working fluids," Energies (Basel), 14 (9) 2548 (2021). doi:10.3390/en14092548.
8) R. Moradi, M. Villarini, E. Habib, E. Bocci, A. Colantoni, and L. Cioccolanti, "Impact of the expander lubricant oil on the performance of the plate heat exchangers and the scroll expander in a micro-scale organic rankine cycle system," Appl Therm Eng, 189 116714 (2021). doi:10.1016/j.applthermaleng.2021.116714.
9) M.-H. Yang, and R.-H. Yeh, "Investigation of the potential of r717 blends as working fluids in the organic rankine cycle (orc) for ocean thermal energy conversion (otec)," Energy, 245 123317 (2022). doi:10.1016/j.energy.2022.123317.
10) X. Zheng, X. Luo, J. Luo, J. Chen, Y. Liang, Z. Yang, Y. Chen, and H. Wang, "Experimental investigation of operation behavior of plate heat exchangers and their influences on organic rankine cycle performance," Energy Convers Manag, 207 112528 (2020). doi:10.1016/j.enconman.2020.112528.
11) Z. Han, H. Zhang, D. Wu, and F. Ma, "Performance optimization for a novel combined cooling, heating and power-organic rankine cycle system with improved following electric load strategy based on different objectives," Energy Convers Manag, 221 113294 (2020). doi:10.1016/j.enconman.2020.113294.
12) Cuk Supriyadi AN, A. Guardi, H. Purnama, K. Herbandono, H. Hermawan, R. Harmadi, Lia Agustina Setyowati, and D. Winarso, "Optimization and analysis of excess heat utilization from an exhaust outlet in a waste incinerator plant : case study

of the hydro drive incinerator, west java, indonesia," Evergreen, 11 (3) 2659–2667 (2024). doi:10.5109/7236905.

13) B.S. Tilley, V.C. Yang, J.C. Baiense, and S. Evans, "Frequency-dependent thermal resistance of vertical u-tube geothermal heat exchangers," J Eng Math, 102 (1) 131–150 (2017). doi:10.1007/s10665-016-9881-7.
14) S.-W. Perng, R.-F. Horng, and H.-W. Wu, "Effect of a diffuser on performance enhancement of a cylindrical methanol steam reformer by computational fluid dynamic analysis," Appl Energy, 206 312–328 (2017). doi:10.1016/j.apenergy.2017.08.194.
15) W. Sun, Y. Liu, M. Li, Q. Cheng, and L. Zhao, "Study on heat flow transfer characteristics and main influencing factors of waxy crude oil tank during storage heating process under dynamic thermal conditions," Energy, 269 127001 (2023). doi:10.1016/j.energy.2023.127001.
16) I.V. Miroshnichenko, and M.A. Sheremet, "Turbulent natural convection heat transfer in rectangular enclosures using experimental and numerical approaches: a review," Renewable and Sustainable Energy Reviews, 82 40–59 (2018). doi:10.1016/j.rser.2017.09.005.
17) J.G.M. Kuerten, C.W.M. van der Geld, and B.J. Geurts, "Turbulence modification and heat transfer enhancement by inertial particles in turbulent channel flow," Physics of Fluids, 23 (12) (2011). doi:10.1063/1.3663308.
18) L. Yuan, S. Zou, Y. Yang, and S. Chen, "Boundary-layer disruption and heat-transfer enhancement in convection turbulence by oscillating deformations of boundary," Phys Rev Lett, 130 (20) 204001 (2023). doi:10.1103/PhysRevLett.130.204001.
19) Y. Menni, A. Azzi, and A. Chamkha, "Enhancement of convective heat transfer in smooth air channels with wall-mounted obstacles in the flow path," J Therm Anal Calorim, 135 (4) 1951–1976 (2019). doi:10.1007/s10973-018-7268-x.
20) H.A. Mohammed, G. Bhaskaran, N.H. Shuaib, and R. Saidur, "Heat transfer and fluid flow characteristics in microchannels heat exchanger using nanofluids: a review," Renewable and Sustainable Energy Reviews, 15 (3) 1502–1512 (2011). doi:10.1016/j.rser.2010.11.031.
21) J.Y. Yoo, "The turbulent flows of supercritical fluids with heat transfer," Annu Rev Fluid Mech, 45 (1) 495–525 (2013). doi:10.1146/annurev-fluid-120710-101234.
22) Mohammad Nurizat Rahman, "Optimisation of solid fuel in-furnace blending for an opposed-firing utility boiler: a numerical analysis," CFD Letters, 14 (9) 89–107 (2022). doi:10.37934/cfdl.14.9.89107.
23) Cahyadi, T. Hidayat, Y. Ahda, and T. Sutardi, "Enhancing energy efficiency of thermal oil system in gas processing plant," in: 2024: p. 020132. doi:10.1063/5.0205761.
24) S.M. Hashemi, and M.A. Akhavan-Behabadi, "An empirical study on heat transfer and pressure drop characteristics of cuo–base oil nanofluid flow in a horizontal helically coiled tube under constant heat flux," International Communications in Heat and Mass Transfer, 39 (1) 144–151 (2012). doi:10.1016/j.icheatmasstransfer.2011.09.002.
25) J. Lee, S. Yoon Jung, H. Jin Sung, and T.A. Zaki, "Effect of wall heating on turbulent boundary layers with temperature-dependent viscosity," J Fluid Mech, 726 196–225 (2013). doi:10.1017/jfm.2013.211.
26) O. Shishkina, R.J.A.M. Stevens, S. Grossmann, and D. Lohse, "Boundary layer structure in turbulent thermal convection and its consequences for the required numerical resolution," New J Phys, 12 (7) 075022 (2010). doi:10.1088/1367-2630/12/7/075022.
27) J. Zhao, J. Liu, H. Dong, W. Zhao, and L. Wei, "Numerical investigation on the flow and heat transfer characteristics of waxy crude oil during the tubular heating," Int J Heat Mass Transf, 161 120239 (2020). doi:10.1016/j.ijheatmasstransfer.2020.120239.
28) T. Wei, and W.W. Willmarth, "Reynolds-number effects on the structure of a turbulent channel flow," J Fluid Mech, 204 57–95 (1989). doi:10.1017/S0022112089001667.
29) A.J. Smits, B.J. McKeon, and I. Marusic, "High–reynolds number wall turbulence," Annu Rev Fluid Mech, 43 (1) 353–375 (2011). doi:10.1146/annurev-fluid-122109-160753.
30) E.E. Michaelides, "Motion of particles in gases: average velocity and pressure loss," J Fluids Eng, 109 (2) 172–178 (1987). doi:10.1115/1.3242640.
31) Q. Chen, M. Wang, N. Pan, and Z.-Y. Guo, "Optimization principles for convective heat transfer," Energy, 34 (9) 1199–1206 (2009). doi:10.1016/j.energy.2009.04.034.
32) Y. Xu, Q. Cheng, X. Liu, Y. Liu, L. Liu, and M. Gao, "Effects of crude oil's variable physical properties on temperature distribution in a shutdown pipeline," Advances in Mechanical Engineering, 9 (5) 168781401770643 (2017). doi:10.1177/1687814017706432.
33) Y. Zhuang, N. Huang, and Y. Jiang, "Effect of volumetric flow rate on heat transfer characteristics of single-fractured rock with different surface morphology and external temperature," Processes, 12 (12) 2821 (2024). doi:10.3390/pr12122821.
34) S. Anitha, K. Loganathan, and M. Pichumani, "Approaches for modelling of industrial energy systems: correlation of heat transfer characteristics

between magnetohydrodynamics hybrid nanofluids and performance analysis of industrial length-scale heat exchanger," J Therm Anal Calorim, 144 (5) 1783–1798 (2021). doi:10.1007/s10973-020-10072-8.

35) J. Ko, N. Takata, K. Thu, and T. Miyazaki, "Dynamic modeling and validation of a carbon dioxide heat pump system," Evergreen, 7 (2) 172–194 (2020). doi:10.5109/4055215.
36) M.U. Shahid, M.M. Khan, and M.N. Shahid, "Numerical Investigation of the Heat Transfer Rate and Fluid Flow Characteristics of Conventional and Triply Periodic Minimal Surface (TPMS)-Based Heat Sinks," in: ICAME 2024, MDPI, Basel Switzerland, 2024: p. 35. doi:10.3390/engproc2024075035.
37) E.S. Rekunenko, and A.B. Garyaev, "The influence of heat transfer fluid temperature on optimal characteristics of the heating convector," J Phys Conf Ser, 1565 (1) 012064 (2020). doi:10.1088/1742-6596/1565/1/012064.
38) L. V. Plotnikov, D.A. Davydov, D.N. Krasilnikov, V.A. Shurupov, and L.E. Osipov, "Experimental Study of Gas Dynamics and Heat Transfer of a Stationary Flow in Exhaust Pipelines with Different Cross-Sectional Shapes," in: 2024: pp. 318–328. doi:10.1007/978-3-031-65870-9_28.
39) N. Kumar, Manoj Kumar Singh, Vinod Singh Yadav, V. Singh, and A. Maheswari, "A comparative analysis of ribs and cans type solar air heater," Evergreen, 10 (3) 1449–1459 (2023). doi:10.5109/7151694.
40) B. Al Zaitone, M. Usman, A. Al-Zahrani, S. Rather, and U. Saeed, "Investigation of convective heat transfer from a high temperature prolate spheroid to moving fluid," Numeri Heat Transf A Appl, 82 (4) 124–136 (2022). doi:10.1080/10407782.2022.2066925.
41) F. Giacalone, F. Vassallo, L. Griffin, M.C. Ferrari, G. Micale, F. Scargiali, A. Tamburini, and A. Cipollina, "Thermolytic reverse electrodialysis heat engine: model development, integration and performance analysis," Energy Convers Manag, 189 1–13 (2019). doi:10.1016/j.enconman.2019.03.045.